Int. J. Multiphase Flow Vol. 14, No. 1, pp. 121–127, 1988
Printed in Great Britain.

0301-9322/88 $3.00 + 0.00

BRIEF COMMUNICATION

GAS DISPERSION PHENOMENA FROM POROUS STIRRING ELEMENTS

C. J. DOBSON
BHP Central Research Laboratories, Shortland, NSW 2307, Australia

N. A. MOLLOY
Department of Chemical & Materials Engineering, University of Newcastle, Newcastle, NSW 2308, Australia

(*Received* 5 *January* 1987; *in revised form* 15 *June* 1987)

INTRODUCTION

Stirring in steelmaking ladles for temperature and composition homogenization is accomplished by the submerged injection of gas through a porous nozzle situated in the ladle base. Extended service of such a nozzle may be obtained by ensuring that the large gas bubbles forming in the liquid steel do so sufficiently distant from the nozzle. Gas will thus be prevented from spreading across the nozzle plane, avoiding associated refractory wear problems due to mechanical erosion and thermal cycling.

The volume of a bubble (V_b) produced on submerged gas injection may be predicted by the Davidson & Schuler (1960) relation

$$V_b = A\, Q^{\frac{6}{5}} g^{-\frac{3}{5}}, \qquad [1]$$

where Q is the gas flowrate in m^3/s and g is the gravitational constant.

It was found that the dimensionless constant A = 1.378 for low-flowrate injection from single nozzles. At higher flowrates the bubble volumes are found to be lower than those predicted by [1] (Wraith & Chalkley 1977; Farias 1982; Li *et al.* 1985). This has been attributed to the gas momentum flux (F_M) assisting the buoyancy force (F_B) in detaching the bubble from the nozzle, thus decreasing its volume at detachment. The rato F_M/F_B was referred to as the "injection number" (Farias 1982), where

$$N_I = C\left[\frac{Q^2}{(r_o^5 g)}\right]^{\frac{2}{5}} \frac{\rho_G}{\rho_L} \qquad [2]$$

and

$$C = (4\pi A^5)^{-\frac{1}{5}}; \qquad [3]$$

r_o is the nozzle radius and ρ_G and ρ_L are the gas and liquid densities, respectively. Under these conditions it was found that A = 1.09.

Isothermal model studies in gas/water systems enable convenient visualization of gas dispersion processes from industrial porous stirring elements at flowrates characteristic of those used in steelmaking processes, if a similar Froude number can be obtained in the model.

Modelling experiments with non-metallic liquids utilizing [2] (Hoefele & Brimacombe 1979; Farias 1982; Dobson 1984) were shown to be valid in representing gas injection into liquid metals through single nozzles. Figure 1 shows the dependence of the measured dimensionless bubble volume on the Froude number for some gas/liquid systems (v_o is the nominal gas velocity at the nozzle exit in m/s and r_o is the nozzle radius).

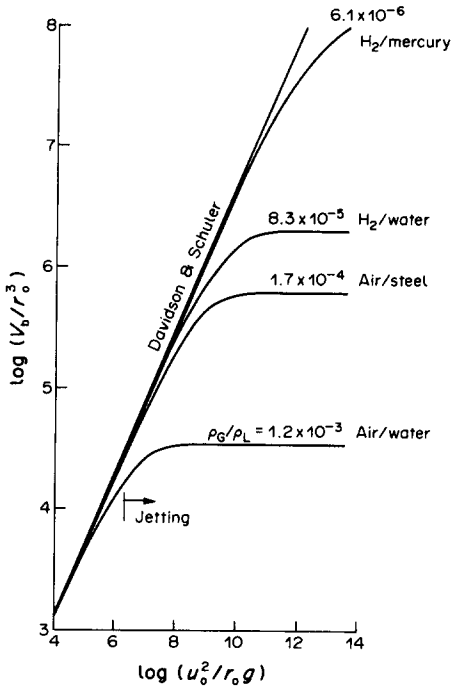

Figure 1. Dimensionless bubble volume as a function of Froude number for different systems [after Farias (1982)].

Previous work on injection through multiple and porous sources has been done by Otero *et al.* (1985), Wraith & Baxter (1970) and Bowonder & Kumar (1970). For high flowrates, up to 0.2 m^3/s, through a series of single adjacent nozzles Otero *et al.* proposed the relation

$$d_{bo} = 0.66\, Q^{0.23}\, d_o^{0.12} \qquad [4]$$

to predict bubble diameter (d_{bo}) in a rising two-phase plane, where d_o is the nozzle diameter. By injecting air into water, Wraith & Baxter (1970) identified four distinct changes in the formation mode of the gas dispersion with increasing gas flowrate through a sintered porous disc. They noted that ultimately large bubbles were formed which grew and enveloped the disc before rising, in a similar way to those formed at single nozzles. Grabner (1983, 1985) postulated that such phenomena could lead to erosion of the disc by thermal and mechanical effects.

EXPERIMENTAL

Characteristics of the porous nozzle elements

The nozzle elements were made using a 100 mm length of an industrial nozzle brick. The nozzles were:

1. "Porous plug" (PP)—a sintered refractory material providing random gas passageways of varying size. The diameter of the element was 75 mm and its porosity about 50% (figure 2a).
2. "Permeable brick" (PB)—a ceramic element with three parallel rows of rectangular orifices provided by steel plates, each orifice being about 5 × 0.5 mm^2, with 7 orifices in each row of 150 mm length (figure 2b).
3. "Multiple hole brick" (MHB)—a 150 mm dia ceramic element with a uniform square array on a 12.5 mm grid of 85 orifices of 1 mm dia (figure 2c).

The nozzles were set into a flat plate in the bottom of a cylindrical Perspex tank of 960 mm dia and 1200 mm height. Helium or air was injected over a range of flowrates up to 0.12 m^3/s and the

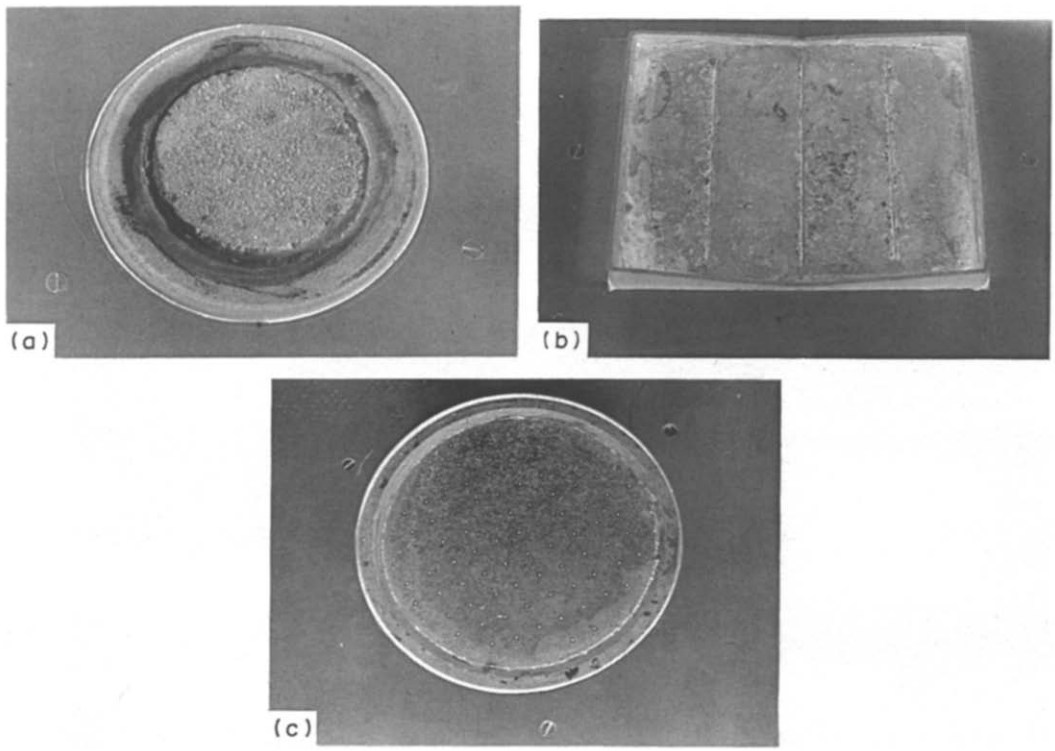

Figure 2. Porous nozzle elements: (a) porous plug (PP); (b) permeable brick (PB); (c) multiple hole brick (MHB).

gas dispersion behaviour was recorded using high-speed cine photography at about 800 pictures/s. Simultaneous continuous video logging included the high-speed experimental segment to enable the general flow pattern and high-speed segment to be related.

RESULTS

Visual observation

Bubble formation and subsequent growth cycles have been reported elsewhere (Davidson & Schuler 1960; Wraith & Chalkley 1977) and no duplication is made here.

On increasing the gas flowrate (for either air or helium) the following four regimes were observed [using the nomenclature of Wraith & Baxter (1970) for the same phenomena]:

(a) Quiescent bubble formation (figure 3a): individual pores operate independently as bubble sources. A steady stream of bubbles then rises. Increasing the flowrate increases the number of sources operating.
(b) Coalescence (figure 3b): on increasing the flowrate some adjacent bubbles coalesce into a foam and again a steady stream of bubbles rises; the first appearance of a cooperative phenomenon.
(c) Pulsation coalescence (figure 3c): increased coalescence into the foam occurs closer to the element until almost all of the bubbles formed at the element are swept into the larger coalesced bubbles. The rising column begins to pulsate with radial excursions of the two-phase envelope.
(d) Blanketing (figure 3d): large bubbles (up to five times the nozzle diameter) grew directly over the element and surrounding plate, effectively forming a gas

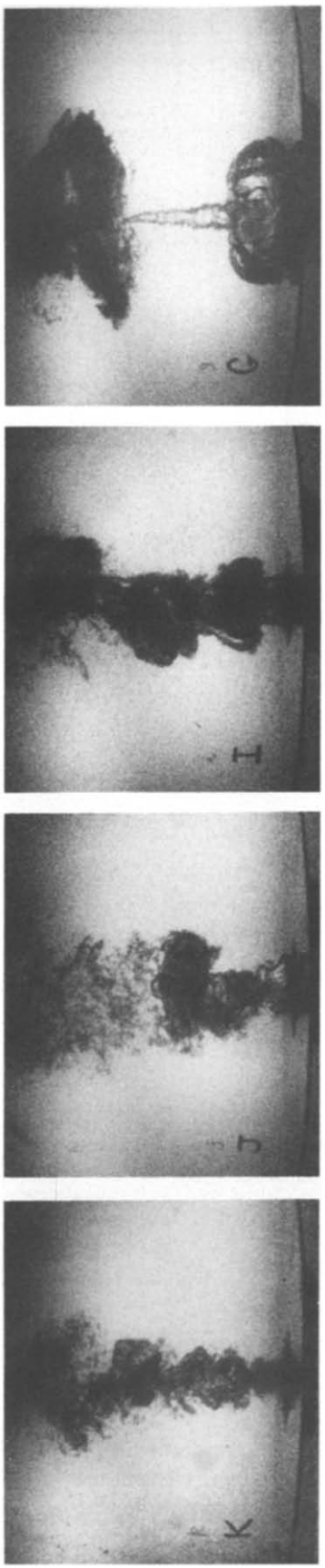

Figure 3. Air injection through the PP. Flow rate (m^3/s): (a) 1.3×10^{-3}; (b) 3.2×10^{-3}; (c) 8.0×10^{-3}; (d) 22.0×10^{-3}.

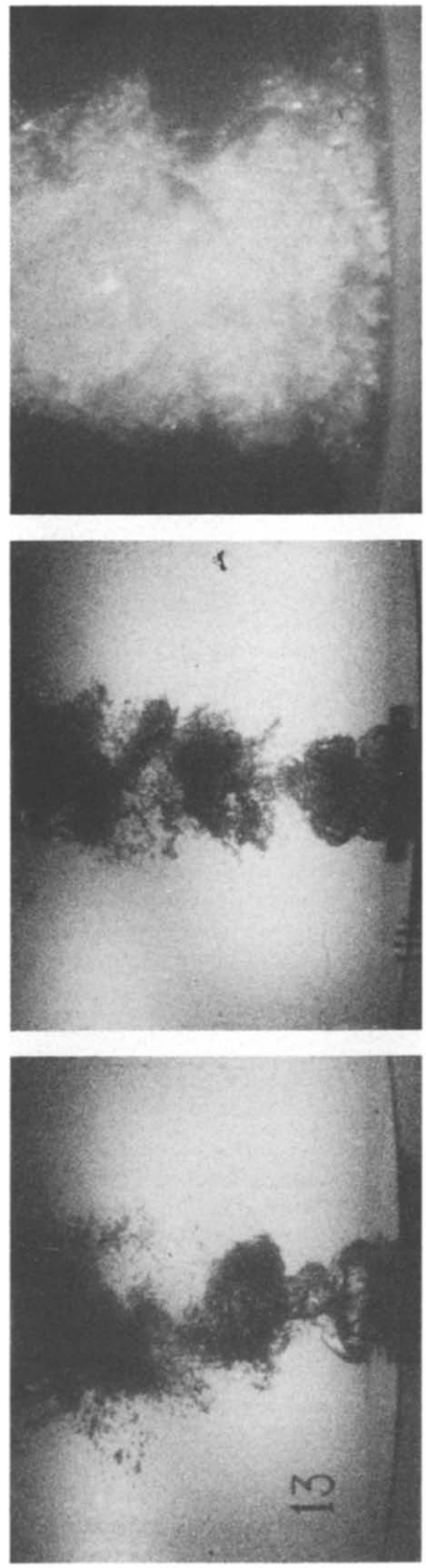

Figure 4. Helium injection through each type of nozzle: (a) PP, flowrate = 4.4×10^{-3} m^3/s; (b) PB, flowrate = 4.9×10^{-3} m^3/s; (c) MHB, flowrate = 4.9×10^{-3} m^3/s.

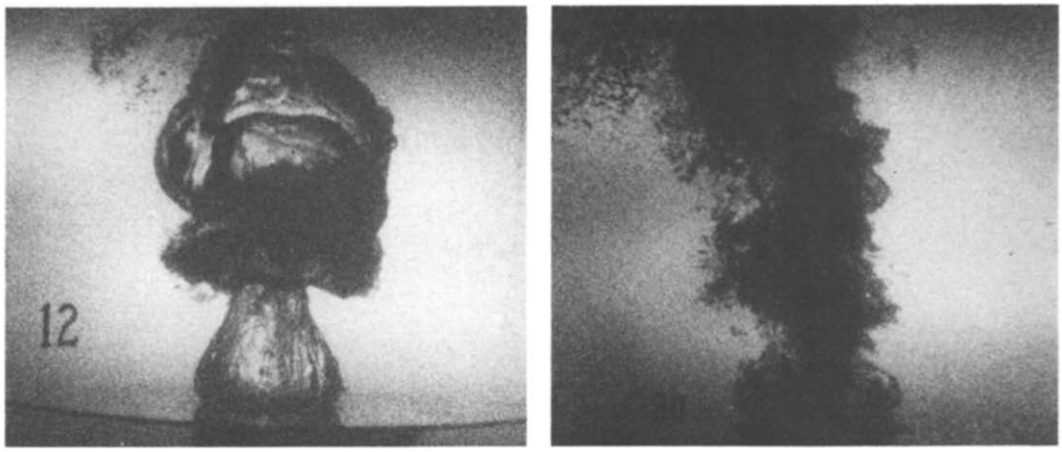

(a) (b)

Figure 5. Helium injection: (a) PP, flowrate = 6.5×10^{-3} m^3/s; (b) MHB, flowrate = 9.2×10^{-3} m^3/s.

blanket. As the bubble shown in the photograph rises it is replaced by in-rushing water until the next bubble "bursts" over the plate repeating the cycle at about 5–7 Hz. Pulsation became more pronounced with increasing flow as bubbles grew in a manner similar to those formed at a single-orifice opening, due to the dominance of the cooperative effect.

Gas dispersion above each type of element is apparently the same about three bubble diameters above the element (figures 4a–c). The large gas-filled envelopes formed by coalescence of the gas bubble streams and jets from the numerous sources of the elements break down into a dispersion of discrete bubbles of much smaller size. The large structure depicted in figure 5a has a transient existence of <0.5 s.

At similar volumetric flowrates it was obsered that blanketing on the PP element was greater than on the PB, extending beyond the element itself and extending over the bottom plate (figures 5a,b). With the MHB element there was little extension beyond the gas delivery area of the element itself. These differences in behaviour are thought to result from a general increase in gas momentum as the delivery area decreases from the PP to the PB to the MHB. The implications of this aspect of the dispersion mode may be significant in interpreting wear and/or build up around operating elements in high-temperature environments.

Using [2] it is possible to simulate ladle stirring for example, 250 Nl/min of argon injected into liquid steel can be simulated by injecting 240 Nl/min of helium into water. The cold model operation at this flowrate is depicted in figures 4a–c for each element. If the wear mechanism is related to mechanical and thermal stress cycling then the PP element would lead to the greatest amount of wear (due to the predominance of blanketing).

Figure 6 relates the size of the initial bubbles to flowrates and compares the proposed relations, [1] and [4], for single-orifice nozzles. The relation by Otero *et al.* (1985), [4], is for an equivalent single nozzle of 138 mm dia. Equation [4] tends to overestimate bubble volume at low flowrates and to underestimate it at high flowrates.

As the large bubbles formed by the cooperative behaviour of the elements rose, a dispersion of liquid drops was generated in them by secondary coalescence beyond the nozzle due to penetration by the following bubble. This is similar to coalescence with single-orifice operations (Wraith & Chalkley 1977). The effect was marked with the MHB element, less so for the PB element and non-existent in the PP element. Resolution of this observed phenomena is the subject of a continuing programme.

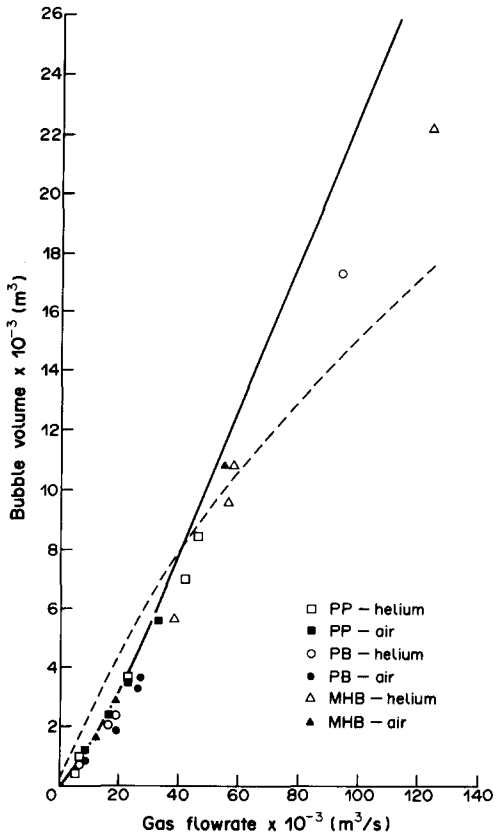

Figure 6. Bubble volume vs gas flowrate—comparison of experimental data with the models of: ——, Davidson & Schuler (1960); – – –, Otero *et al.* (1985).

CONCLUSIONS

Large gas bubbles form during injection from porous nozzle elements, with diameters of up to 0.5 m from elements of about 0.075 m dia.

Gas dispersion at a height above the element of about three bubble diameters appears the same, regardless of the geometry of the source nozzle.

Bubble volume from porous nozzle elements may be estimated by the Davidson–Schuler (1960) relation up to flowrates of 2.3 m^3/s, with a tendency to overestimate at the maximum flowrate investigated.

The size and structure of the bubbles produced indicate the necessity of further evaluation particularly in industrial situations of the flowrate–wear relation.

Acknowledgement—The authors gratefully acknowledge the Broken Hill Proprietary Co. Ltd for permitting publication of this work.

REFERENCES

BOWONDER, B. & KUMAR, R. 1970 Studies in bubble formation—IV: bubble formation of porous discs. *Chem. Engng Sci.* **25,** 25–32.

DAVIDSON, J. F. & SCHULER, B. O. G. 1960 Bubble formation of an orifice in a liquid. *Trans. Instn chem. Engrs* **38,** 335–342.

DOBSON, C. J. 1984 Fluid dynamics of heat transfer in submerged injection of gases into liquid metals for refining. Ph.D. Thesis, Imperial College, London.

FARIAS, L. R. 1982 Fluid mechanics of submerged gas injection in metallurgy. Ph.D. Thesis, Imperial College, London.

GRABNER, B. E. 1983 Installation and behaviour of porous plugs with directed porosity in LD vessels and ladles. Paper presented at *Scaninject III Conf.*, Luleå, Sweden, pp. 8–23.

GRABNER, B. E. 1985 Applications and wear of porous plugs in secondary metallurgy. *Radex Rdsch* **3,** 581–610.

HOEFELE, E. O. & BRIMACOMBE, J. K. 1979 Flow regimes in submerged gas injection. *Met. Trans.* **10B,** 631–648.

LI, W., CHAMBERS, A. J. & MOLLOY, N. J. 1985 A modified mechanism of bubble blowing from a nozzle. Extraction Metallurgy Report EMR 1/85, Univ. of Newcastle, NSW.

OTERO, Z., TILTON, J. N. & RUSSELL, T. W. 1985 Some observations on flow patterns in tank type systems. *Int. J. Multiphase Flow* **11,** 583–589.

WRAITH, A. E. & BAXTER, R. T. 1970 Transitions in the bubble formation mode of a submerged porous disc. *Chem. Engng Sci.* **25,** 1244–1247.

WRAITH, A. E. & CHALKLEY, M. E. 1977 Tuyere injection for metal refining. In *Advances in Extractive Metallurgy, Proc. IMM Symp., London* (Edited by JONES, M. J.), pp. 27–33.